Rotational Relaxation in Supercritical Carbon Dioxide Revisited: A Study of Solute-Induced Local Density Augmentation

Janet L. deGrazia and Theodore W. Randolph*

Department of Chemical Engineering, University of Colorado at Boulder, Boulder, Colorado 80309-0424

James A. O'Brien

PTT, Inc., 305 Madison Avenue, Suite 1425, New York, New York 10017

Received: October 16, 1997; In Final Form: December 16, 1997

We examine the rotational diffusion of copper 2,2,3-trimethyl-6,6,7,7,8,8,8-heptafluoro-3,5-octanedionate in liquid solvents and supercritical carbon dioxide using electron paramagnetic resonance spectroscopy. We find that rotational correlation times in the CO_2 were considerably larger than those predicted by Stokes−Einstein−Debye theory at regions close to the critical density, a finding similar to that of Heitz and Bright. Local density augmentation was quantified using a model developed by Anderton and Kauffman. At low bulk densities, we find extraordinarily high local density enhancements, with local densities over four times higher than those of the bulk, while at higher bulk densities, the apparent local density approaches that of the bulk. Although consistent with the results reported by Heitz and Bright, apparent local densities far surpassed those of the liquid solvents, a physically unreasonable result. When local densities are calculated using a molecular dynamics approach, the enhancement is less than that shown experimentally and compares reasonably to liquid densities. A clear maximum for this enhancement at subcritical densities is shown for the first time in these types of simulations. Reaction rate constants for Heisenberg spin exchange from experiments are found to be consistently higher than those predicted by theory, indicating a likely contribution of solute−solute local density enhancements to the observed slowing of molecular rotation in supercritical CO_2.

Introduction

Supercritical fluids offer an attractive alternative to current solvent choices due to their gaslike viscosities and liquidlike solvation power. Since their solvent properties are highly sensitive to small changes in pressure or temperature, especially in the immediate vicinity of the critical point, they are of great interest for both separation[1] and reaction[2] processes.

Experiments have shown solute−solvent interactions in supercritical fluids to be higher than those in homogeneous liquids, causing effective local densities of solvent around solutes to be several times higher than bulk density.[3−13] This can affect reactions through both the rate constants[11,14] and the local concentrations of the reactants.[15,16]

Experimental and theoretical approaches have been used to study these local density enhancements. UV,[7,9,10] electron paramagnetic resonance (EPR),[11] and fluorescence spectroscopy[3,4,6,17] have been used, as well as photoionization techniques.[18,19] Integral equation approaches[20−22] as well as fluctuation theory[23] and molecular dynamics[24,25] have been used to calculate excesses of solvent molecules. The physical interpretation of these clusters can be attributed to two effects: indirect solute−solvent interactions, which cause large partial molar volumes, and direct enhancements, which are observed spectroscopically and which arise from direct solute−solvent correlations that extend over the range of the solute−solvent interaction potential.[26]

There is also experimental and theoretical evidence of solute−solute local density enhancements, although it is difficult to separate their effects from solvent−solute interactions. Electron paramagnetic resonance[27] and FT-IR spectroscopy[28,29] support the existence of solute−solute clustering, as do molecular dynamic simulations[30] and integral equation calculations.[21,31,32]

Measurement of rotational relaxation can be an ideal method to investigate solvent−solute interactions in supercritical fluids. A model that relates solvent−solute forces to solute shape and motion can provide information about the association of solvent with solute. One such model yields the Stokes−Einstein−Debye (SED) equation[33]

$$\tau = \eta V/kT \tag{1}$$

where τ is the rotational correlation time, η is the bulk solvent viscosity, V is the volume of the solute, k is Boltzmann's constant, and T is the absolute temperature. This model assumes that the solute is spherical and very large compared to the surrounding solvent molecules; therefore, the solvent adjacent to the rotating particle rotates with it.

Although this model works well for those systems that are so described, there are a number of systems for which it is inappropriate. These include systems with solutes that are not spherical or not very large with respect to their solvent. A number of approaches have been proposed to address the SED model's shortcomings. A modified version of the SED equation is often used[34]

$$\tau = \frac{\eta V}{kT} f_{\text{stick}} C \tag{2}$$

where f_{stick} is a dimensionless frictional coefficient related to

* Corresponding author. Telephone: (303) 492-4776. Fax: (303) 492-4341. E-mail: randolph@pressure.colorado.edu.

S1089-5639(97)03373-2 CCC: $15.00
Published on Web 02/14/1998

solute shape and C is a dimensionless parameter that depends on boundary conditions. The SED equation describes a spherical solute with $f_{stick} = 1$ and stick boundary conditions with $C = 1$. Theoretical suggestions for treatment of these two parameters have been offered where $f_{stick} = 1$ and C varies between C_{slip} and 1[35−37], where C_{slip} is the boundary condition for a rotating particle that displaces the surrounding fluid and, in turn, exerts no drag force on the particle, or where $f_{stick} \neq 1$ and $C = 1$.[38,39] Gierer and Wirtz[40] developed an expression for C that describes the case of a spherical probe surrounded by concentric shells of solvent, and Dote et al.[34]developed a theory based on the existence of free volume described in terms of the bulk properties of the fluid.

A number of experimental approaches using rotational relaxation processes have been used to describe solvent−solute interactions in supercritical fluids. For example, Evilia et al.[41] measured the rotational correlation time of several small molecules dissolved in supercritical fluids using ^{14}N NMR spectroscopy and found that, at the low viscosity typical of supercritical fluids, the reorientation time was close to the inertial limit. Bowman et al.[42] examined the rotational relaxation of D_2O in Xenon and CO_2 and found free rotation in Xe at all densities but hindered rotation in CO_2 as the density increased. They attributed these differences to lack of electrostatic interactions between solvent and solute in Xe but considerable dipole−quadrapole interactions in CO_2. Howdle and Bagratashvili[43] looked at the rotational Raman spectrum of hydrogen dissolved in supercritical CO_2 and attributed the resulting line broadening to solvent−solute interactions. Chen et al.[44]reported on the rotational and angular momentum correlation times of naphthalene dissolved in CO_2. Their results indicated that there is a substantial solvent density augmentation but that it does not cause measurable changes in the rotational properties of the solute.

Other research led to attempts to quantify these solvent−solute interactions. Betts et al.[45] used fluorescence anisotropy and lifetime measurements to determine the rotational correlation time in supercritical N_2O. They then used the SED equation to determine a volume and thereby could quantify the lower and upper volume limits of a solvent cluster around the solute. They found that the volume of the cluster is maximal near the critical point, scales as the isothermal compressibility, and decreases with increasing pressure, regardless of the rotational diffusion model used.

Anderton and Kauffman[46] used the expression

$$\tau = \frac{\eta V}{kT} f_{stick} C + \tau_0 \tag{3}$$

where τ_0 accounts for the finite rotational relaxation at zero viscosity and

$$f_{stick} = \frac{2(A^2+1)(A^2-1)^{1.5}}{3A\{(2A^2-1)\ln[A+(A^2-1)^{0.5}] - A(A^2-1)^{0.5}\}} \tag{4}$$

where A is the ratio of the longitudinal solute dimension to the axial solute dimension. For diphenylbutadiene in *n*-alcohols, the authors used an expression based on the Dote−Kivelson−Schwartz model[34] to determine C. The solvent molar volume was used as a measure of the free volume per solvent molecule. Anderton and Kauffman extended this model to supercritical fluids by including two variables that depend on local density[47]

$$\tau = \frac{\eta(\rho_L)V}{kT} f_{stick} C(\rho_L) + \tau_0 \tag{5}$$

so that both the viscosity term and the boundary condition factor reflect the influence of the local solvent density, ρ_L. The viscosity term was written in terms of density in the method of Jossi et al.,[48] and the boundary condition was found using a modification of Dote et al.'s[34] equation that reflected the compressible nature of a supercritical fluid. The local density was related to the bulk solvent density and the solvent−solute pair distribution function, $g_{12}(r)$ through the equation

$$\rho_L(r) = \rho(1 + F(g_{12}(r))) \tag{6}$$

where F is an integral equation in $g_{12}(r)$ (undefined by Anderton and Kauffman) over the spatial coordinates and describes the excess solvent density in the region of a solute molecule.

More recently, Heitz and Bright[49] have examined the rotational reorientation times of *N*,*N*′-bis(2,5-*tert*-butylphenyl)-3,4,9,10-perylenecarboxodiimide (BTBP) in liquid solvents and compared them to rotational reorientation times in supercritical fluids. They found that rotational reorientation times deviated from those predicted from hydrodynamic theory near the critical point, and they used the model developed by Anderton and Kauffman[47] to quantify the degree of local fluid density around the solute. Local densities were estimated to be extraordinarily large, substantially exceeding liquid density.

Finally, Heitz and Maroncelli[50] reexamined the rotational dynamics of BTBP and investigated two other solutes, 1,3,6,8-tetraphenylpyrene (TPP) and 9,10-bis(phenylethynyl)anthracene in supercritical CO_2 using picosecond fluorscence anisotropy decay measurements. They found, contrary to the previous work of Heitz and Bright[49] that TPP and BTBP exhibited rotation times consistent with hydrodynamic theory, although solubility concerns prevented them from studying reduced densities below 1.2 for TPP and BTBP.

In this article, we examine the rotational diffusion of copper 2,2,3-trimethyl-6,6,7,7,8,8,8-heptafluoro-3,5-octanedionate (Cufod) (see Figure 1) in liquid solvents and supercritical carbon dioxide using EPR spectroscopy. Previous investigators analyzed rotational correlation times in terms of local solvent−solute density enhancements. We will show that without considering solute−solute local density enhancement such analysis produces unphysical results. In addition, we model our system as a Lennard-Jones fluid and perform molecular dynamics calculations to quantify the extent of local density enhancement. Finally, Heisenberg spin exchange measurements will be used to provide insight into the effect of solute−solute local density enhancements on solute rotational relaxation in supercritical solvents.

Cufod is known to be quite soluble in supercritical carbon dioxide[51] due to its highly fluorinated structure and has been previously investigated as a potential candidate for metal extraction.[52] Because of highly anisotropic A values, where A is the hyperfine coupling constant, EPR spectra of Cufod are sensitive to rotational motion even in fluids of low viscosity such as supercritical CO_2. EPR gives us the ability to examine both solvent−solute interactions through rotational correlation times and solute−solute interactions through Heisenberg spin exchange. Since Cufod is soluble even at relatively low CO_2 densities, we are able to examine solvent−solute interactions and calculate local density enhancements at lower reduced densities than either Heitz and Bright[49] or Heitz and Maroncelli[50] were able to attain.

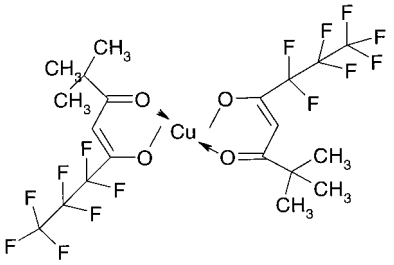

Figure 1. Molecular structure of copper 2,2,3-trimethyl-6,6,7,7,8,8,8-heptafluoro-5,5-octanedionate (CuFod).

Materials and Methods

Cufod was purchased from Gelest and used as received. Instrument grade CO_2 was obtained from Air Products and passed through an oxygen scrubber (Labclear) and a reactor filled with P_2O_5 to further purify it for EPR experiments. Linde bone dry grade (99.8%) CO_2 was used without further purification for solubility experiments. All liquid solvents were technical grade.

Solubility measurements were made using the method of Lemert et al.[53] in a 28 mL stainless steel variable-volume view cell containing a sapphire window. Cufod (10 or 20 mg) was placed in the cell with 10 mL of carbon dioxide at 3000 psi. A piston was used to vary the volume and therefore the pressure. Measurements were made at constant weight fraction for temperatures between 35 °C and 60 °C. The pressure and temperature were measured to ±0.2 bar and ± 0.2 K, respectively.

X-band EPR spectra were recorded in a Bruker ESP300 EPR spectrometer. A high-pressure closed-loop recirculating cell as described earlier[11] was used for the supercritical CO_2 experiments. The system was modified in the following fashion. All tubing and crosses were constructed of PEEK (Alltech), as was the reactor (Upchurch), to avoid reaction of Cufod with stainless steel.[54] PEEK has a characteristic EPR signal that was subtracted from the recorded spectra. Cufod was added to the system in the reactor, and oxygen was then purged from the system as described by Carlier and Randolph.[11] Temperatures in the EPR cavity were measured with a thermocouple, and the cell was thermostated to ±0.1 K using a liquid nitrogen boil-off and a Eurotherm temperature controller.

EPR measurements for the supercritical carbon dioxide were made either at constant Cufod concentration or at constant Cufod mole fraction. The first method involved placing a known concentration of Cufod in the reactor, then pressurizing the system to approximately 60 bar with deoxygenated CO_2. The system was allowed to stabilize, and an EPR spectrum was recorded. The pressure was then increased by adding fresh CO_2 from the syringe pump, and the process was repeated. The second method involved pressurizing the system to approximately 150 bar after the sample was introduced, then allowing the system to stabilize, and recording an EPR spectrum. A lower pressure was then set by allowing both Cufod and CO_2 to escape through a micrometering valve, thus maintaining constant mole fraction. Both methods gave equivalent results.

Since the hydrodynamic radius of Cufod had not been reported previously, rotational diffusion times (D_{rot}) were measured in a series of liquid solvents, and an average hydrodynamic radius was determined. Measurements in liquid solvents were done at 296.1 K and used the following procedure: all solvents were dried over molecular sieves for 24 h. 1 mM Cufod was added to each solvent, and about 1 mL was placed in a glass tube (volume ca. 2 mL). To remove oxygen, the tube was frozen in liquid N_2, thawed, frozen again and then thawed, and finally frozen under vacuum and sealed while frozen. The EPR spectrum was recorded after allowing the temperature in the EPR cell to stabilize.

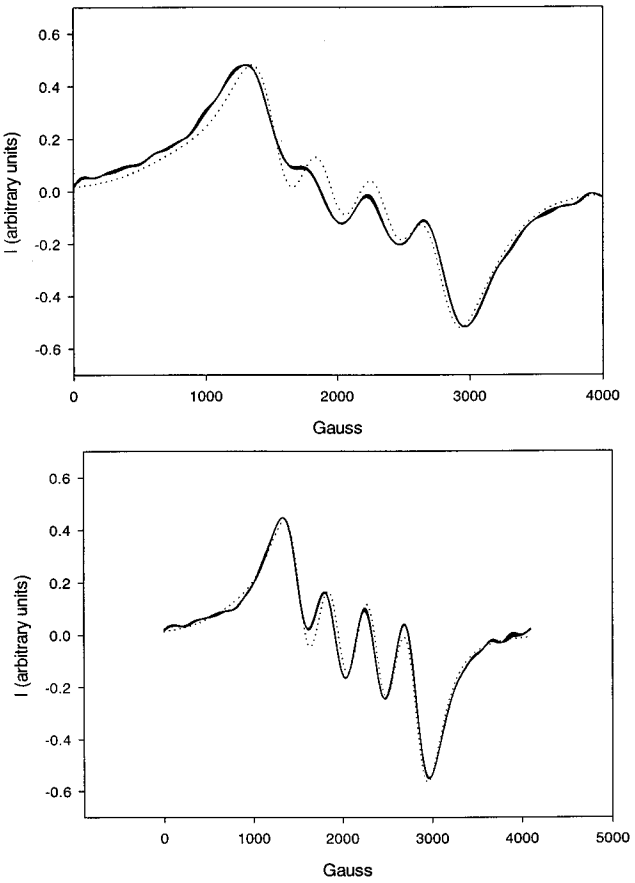

Figure 2. Simulation (dashed line) of the EPR spectrum (straight line) of Cufod in supercritical carbon dioxide. (a) Reduced density = 0.7. (b) Reduced density = 1.58.

All EPR spectra were recorded using a modulation amplitude of 1.01 G, 100 kHz modulation frequency, a time constant of 0.16 ms, and a microwave power of 10 mW. The center field was set at 3267.8 G. Each recorded spectrum was the average of 16 20 s, 800 G scans.

Digitized spectra were transferred to a Hewlett-Packard 720 workstation. Simulated EPR spectra were fit to experimental spectra using fitting programs[55] based on the EPR simulation code of Schneider and Freed.[56] The g values for square planar Cu^{2+} of 2.2550, 2.0606, and 2.0569 used in the program were obtained from the single-crystal structure of bis(3-methylpentane-2,4-dionato) copper(II) because of its structural similarity to Cufod.[57] The A values of 145.5, 29, and 29 G were obtained from EPR observations of copper(II) bisacetylacentonate.[58] The parameters used for the fit were two rotational diffusivities, D_{xy} and D_{zz}, and the Heisenberg spin exchange rate per molecule. D_{rot} was calculated from $(D_{xy}D_{zz})^{1/2}$. The rotational correlation time, τ, was then obtained through the relation[59]

$$\tau = D_{rot}/6 \qquad (7)$$

Figure 2 shows typical experimental and fitted spectra. Agreement between the two was good at all pressure and temperatures.

D_{rot} was determined for Cufod in supercritical CO_2 for reduced densities from 0.7 to 1.8, and hydrodynamic radii were estimated from the SED equation and compared with those determined in the liquid solvents. Effective viscosities were

TABLE 1: Lennard-Jones Parameters Used in Simulations

	σ_{ij} (Å)	ϵ_i/k_j (K)
CO_2-CO_2	4.416	192.25
CO_2-Cufod	8.308	405.67
Cufod−Cufod	12.2	856

calculated using the hydrodynamic radius determined in liquid solvents and compared to those of the bulk as determined from the equation of Jossi et al.,[48] and local densities were determined and contrasted with bulk densities.

Molecular dynamics simulations were carried out as described by O'Brien et al.[60] by approximating Cufod and carbon dioxide as spherical molecules, each characterized by Lennard-Jones (L-J) size and energy parameters σ and ϵ (Table 1). L-J parameters for carbon dioxide ($\sigma = 4.416$ Å, $\epsilon/k = 192.25$ K) were taken from Reid, Prausnitz, and Sherwood.[61] The group contribution method of Ambrose, Joback, and Fedors[62] was used to estimate parameters for Cufod. A check of the L-J parameters shows that the ratio σ_{22}/σ_{11} is close to the cube root of the ratio of molecular masses of Cufod to CO_2 (2.76 as opposed to 2.46, respectively).

The following modifications to the method of O'Brien et al.[60] were made. The minimum cutoff value, r_c, was $2.8\sigma_{12}$, which was equivalent to $5.268\sigma_{11}$ for our system. Infinite dilution was modeled using a single solute molecule in 1199 solvent molecules, so each of our production simulations was for 1200 molecules, which corresponds to a Cufod mole fraction of about 0.0008. All of our runs were at a dimensionless temperature $T^* = 1.323$ (in reduced solvent units), which corresponds to a reduced temperature of $T_r = 1.01$, using the best available value of $T_c = 1.31$ for the L-J fluid.[63]

We carried out simulations over a range of densities chosen to bracket the critical density of $\rho^* = 0.31$. For each density, microstructural information in the form of the radial distribution functions, $g_{11}(r)$ and $g_{12}(r)$ were computed.

We computed the local density enhancement $\rho^{local}(r)/\rho^{bulk}$ from the modified partial fluctuation integral G'_{12}

$$\frac{\rho^{local}}{\rho^{bulk}}(r) = 1 + \frac{3G'_{12}}{\rho^{bulk}\,4\pi(r^3 - r^3_{min})} \tag{8}$$

where

$$G'_{12} \equiv 4\pi\rho^{bulk}\int_{r_{min}}^{r} r^2[g_{12}(r) - 1]\,dr \tag{9}$$

and r_{min} is the separation at which g_{12}, the solute−solvent radial distribution function, first becomes significantly nonzero (here nearly independent of density at $r = 1.69\sigma_{11}$).[25] Local density enhancements were calculated for radial values corresponding to the first, second, third, and fourth solvent shells, i.e., $r = 2.69\sigma_{11}$, $3.69\sigma_{11}$, $4.69\sigma_{11}$, and $5.69\sigma_{11}$.

Results and Discussion

Rotational diffusivities were obtained for Cufod in non-hydrogen-bonding liquid solvents. Equation 3 for rotational correlation time was then used to find the hydrodynamic radius of the copper solute in the liquid solvents. The method of Dote et al.[34] was used to determine C, which was 1, corresponding to sticky boundary conditions. However, since Cufod is not completely spherical, the solute shape-dependent parameter f_{stick} was calculated from eq 4. On the basis of crystallographic data taken from a similar molecule, Cu(fod)PMe_3,[64] A can be estimated to be 1.3 and f_{stick} is then calculated as 1.1 using eq 4. The data for rotational correlation times in liquid solvents

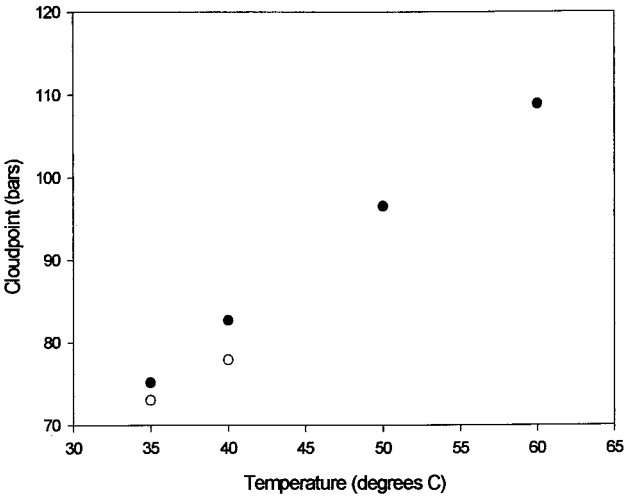

Figure 3. Cloud points of Cufod in carbon dioxide at various temperatures: (●) weight fraction Cufod = 0.01, (○) weight fraction Cufod = 0.005.

TABLE 2: Measured Hydrodynamic Radii of Cufod in Different Liquid Solvents

liquid solvents	viscosity[68] (cp)	rotational correlation time (ps)	hydrodynamic radius (Å)
pentane	0.224	176	7.22
hexane	0.294	182	6.75
heptane	0.400	183	6.11
octane	0.540	184	5.55
benzene	0.600	211	5.83
m-xylene	0.620	230	6.07
nonane	0.670	260	6.29
methylcyclohexane	0.680	263	6.30
ethylbenzene	0.691	274	6.40
o-xylene	0.810	301	6.35

was extrapolated to zero viscosity to obtain τ_0, which was found to be 90 ps. As a cross-check τ_0 was calculated from[65]

$$\tau_0 = \frac{2\pi}{9}\left(\frac{I}{kT}\right)^{0.5} \tag{10}$$

where I is the moment of inertia, obtaining a value of 96 ps. This value is high compared to values found by other authors, such as Heitz and Bright,[49] who found a value of 8.7 ps for BTBP,[49] and Anderton and Kauffman,[47] who determined a τ_0 of 2.9 ps for *trans*-4-(hydroxymethyl)stilbene and 3.7 ps in *trans,trans*-1,4-diphenylbutadiene. However, fluorine atoms on Cufod increase its moment of inertia and therefore τ_0.

Table 2 shows the measured hydrodynamic radii of Cufod in the different liquid solvents. The average hydrodynamic radius for Cufod in 10 liquid solvents was 6.2 ± 0.5 Å, which compares favorably with the estimated Lennard-Jones radius of 6.1 Å.

The solubility of Cufod in CO_2 was then determined. Cloud point measurements (Figure 3) show that weight fractions of 0.01 and 0.005 are completely soluble at the operating conditions used in this study. Care was taken that the weight fraction of Cufod remained at 0.003 or less at all times.

Rotational correlation times were then measured for the Cufod in carbon dioxide at supercritical conditions. Since bulk viscosities for the CO_2 at these pressures (70−160 bar) are much lower than those of the liquid solvents, one would expect the rotational correlation times to be correspondingly smaller. However, that was not the case. Rotational correlation times were considerably larger than those predicted by eq 3, as is

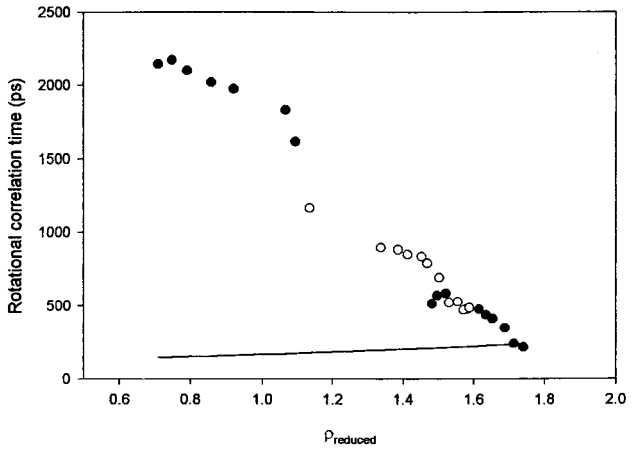

Figure 4. Rotational correlation times of Cufod in supercritical carbon dioxide as a function of density as measured by EPR: (●) Experimentally measured rotational correlation times at $T = 313.1$ K, (○) Experimentally measured times at $T = 308.1$ K, (—) Rotational correlation times as predicted from eq 3 using a hydrodynamic radius of 6.2 Å.

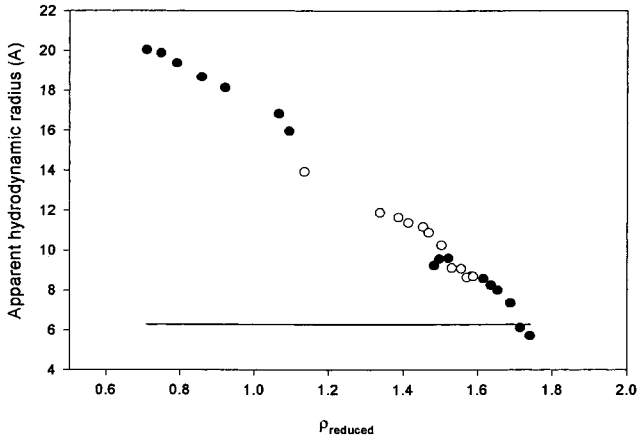

Figure 5. Apparent hydrodynamic radius of Cufod measured in supercritical CO_2 compared with the radius measured in liquid solvents: (●) $T = 313.1$ K, (○) $T = 308.1$ K, (—) radius = 6.2 Å as measured in liquid solvents.

apparent from Figure 4. Using these rotational correlation times and viscosities calculated by the method of Jossi et al.,[48] the apparent hydrodynamic radius for Cufod in supercritical CO_2 was calculated using eq 3. Figure 5 compares apparent hydrodynamic radii at reduced densities of 0.7−1.8 at two different temperatures ($T_r = 1.01$ and $T_r = 1.03$) with the radius calculated from the liquid solvents, i.e., 6.2 Å. At bulk densities which approach liquidlike densities, the apparent hydrodynamic radius approaches that observed in liquid solvents. However, at lower densities, the apparent radius is over three times that seen in liquids.

An alternative analysis assumes a hydrodynamic radius of 6.2 Å as calculated from the liquid solvents and calculates an effective local viscosity using eq 3. This can be compared to the bulk viscosity calculated by the method of Jossi et al.[48] Again, as shown in Figure 6, the apparent local viscosity approaches that of the bulk at higher densities but shows marked deviations in the lower density region.

Following Heitz and Bright,[49] we then used the model developed by Anderton and Kauffman[47] to quantify the degree of fluid density augmentation surrounding our solute. This model assumes that the solute moves independently from the solute−solvent cluster. Assuming a hydrodynamic radius of 6.2 Å, we used eq 3 to determine the effective local viscosity.

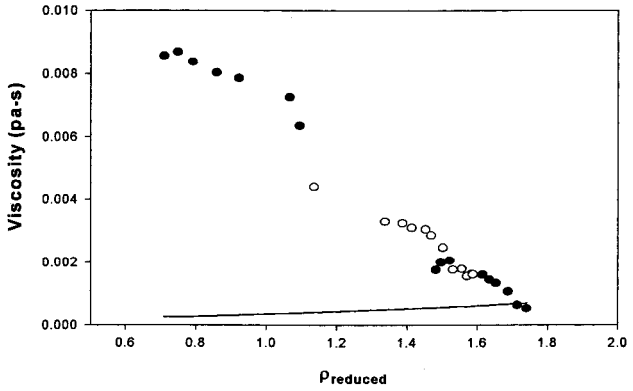

Figure 6. Apparent local viscosity compared to the bulk viscosity as a function of reduced density: (●) $T = 313.1$ K, (○) $T = 308.1$ K, (—) bulk viscosity predicted by method of Jossi et al.

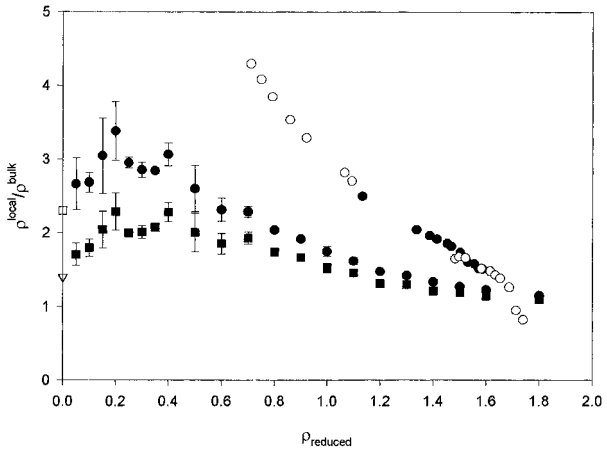

Figure 7. Dimensionless density enhancement as a function of reduced density for two different radial positions obtained through molecular dynamics simulations compared to experimental values as calculated from the Anderton−Kauffman model (eq 6): (▽) analytical calculation for low-density limit at $r = 2.69\sigma_{11}$, (■), (with error bars showing 95% confidence intervals) molecular dynamics simulation for $r = 2.69\sigma_{11}$, (□) analytical calculation for low-density limit at $r = 3.69\sigma_{11}$, (●, with error bars) molecular dynamics simulation for $r = 3.69\sigma_{11}$, (●) experimental values at $T = 308.1$ K, (○) − experimental values at $T = 313.1$ K.

Using the method of Jossi et al.,[48] we calculated the effective local density. Then eq 6 allowed us to compute $F(g_{12}(r))$ where F is an unspecified function related to integrals over $g_{12}(r)$ and is a measure of local density augmentation.

We next turned to molecular dynamics to quantify our local density enhancement, and provide, perhaps, a more realistic model for $F(g_{12}(r))$. Computed local density enhancements for $r = 2.69\sigma_{11}$ and $r = 3.69\sigma_{11}$, which correspond to the first and second solvent shell, respectively, are shown in Figure 7. The results from the EPR experiments, nominally taken at the same temperature, are also shown. While features are similar, the experimental local density enhancement is considerably larger than the simulated one in the lower density regions. This was also seen earlier.[60] However, our computed results show a distinct maximum in local density enhancement that occurs at a reduced density of approximately 0.25, which had not been seen before. Both O'Brien et al.[60] and Knutson et al.[25] show only a muted maximum at best.

It is instructive to compare the various results for $F(g_{12}(r))$ obtained by ourselves as well as data obtained by Heitz and Bright,[49] both using the Anderton and Kauffman model[47] to

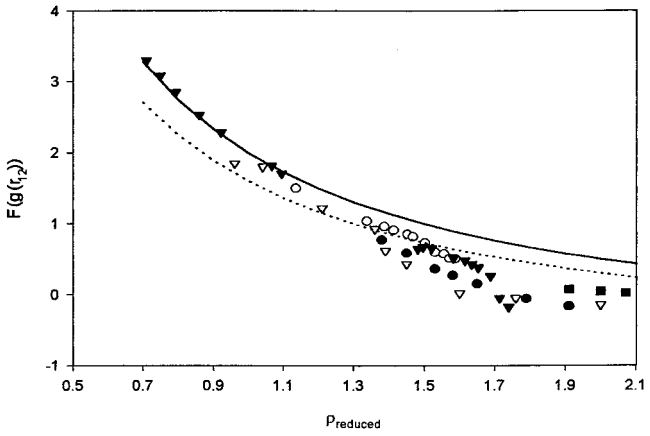

Figure 8. Comparison of $F(g_{12}(r))$ using density augmentations acquired from different sources: (▼) Cufod in CO_2 at $T = 313.1$ K; (○) Cufod in CO_2 at $T = 308.1$ K; (▽) BTBP in CF_3H; (●) BTBP in CO_2; (■) BTBP in C_2H_6; (—) $F(g_{12}(r))$ calculated for $\rho_r = 3$, the upper limit for validity of correlation of Jossi et al.; (- - -) $F(g_{12}(r))$ calculated for $\rho_r = 2.6$, the upper limit for validity of correlation of Vesovic et al. BTBP data taken from Heitz and Bright.[49]

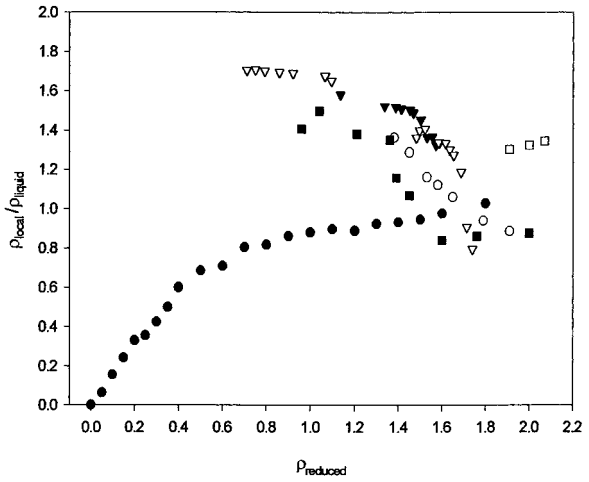

Figure 9. Apparent local density compared to liquid densities as a function of reduced density: (●) MD simulations at $r = 2.69\sigma_{11}$, (○) BTBP in CO_2, (▼) Cufod in CO_2 at $T = 308.1$ K, (▽) Cufod in CO_2 at $T = 313.1$ K, (■) BTBP in CF_3H. (□) BTBP in C_2H_6. BTBP data taken from Heitz and Bright.[49]

obtain density augmentation (Figure 8). At higher densities, as the apparent local density approaches that of the bulk, we find good agreement between all the approaches. Unfortunately solubility considerations limited the results of Heitz and Bright[49] so we are not able to compare experimental points at lower densities.

Analysis of both our and Heitz and Bright's[49] experimental data by the method of Anderton and Kauffman[47] yields local densities that are unphysically high. For illustration, Figure 9 shows the measured local density normalized by the solvent's liquid density at room temperature as a function of reduced density. Although the simulated data approach the limit of liquid density without quite surpassing it, the experimental local density enhancements, when analyzed by the method of Heitz and Bright,[49] exceed the density of liquid solvents (in some cases by over 60%): clearly an unphysical result.

Bulk density increases monotonically with pressure, and the local density should behave in a similar fashion. However, experimental local densities are not monotonic in pressure, an unphysical result. When our data from the molecular dynamics simulation are treated the same way, the local densities increase monotonically as expected.

A possible reason for the unphysical densities that result from the method of Anderton and Kauffman[47] as applied by Heitz and Bright[49] is that the viscosity−density relationship of Jossi et al. is not adequate. Jossi et al.[48] report that their correlation is valid up to $\rho_r = 3$. Most of the reduced local densities found here and by Heitz and Bright[49] lie outside or very close to this range of validity (Figure 8). Heitz and Maroncelli[50] used a different correlation for viscosity determination, that of Vesovic et al.[66] When we reexamined our data using this method, we got similar unphysical results. However, this correlation is valid to $\rho = 1200$ kg/m^3, or a reduced density of approximately 2.6, and again most of results lie outside of this range (see Figure 8).

Although viscosity correlations may lack accuracy very near the critical point, their deficiencies are not sufficient to explain the unphysical results resulting from this analysis. Therefore, the possibility of solute−solute interactions was weighed. Since such simple systems as Lennard-Jones molecules show enhanced solute−solute densities in this region, it should be anticipated that solute−solute interactions in our more complex system could be larger. While solute−solute interactions themselves

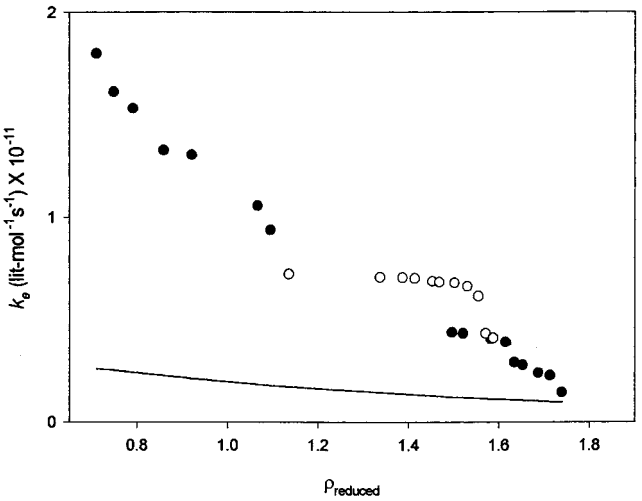

Figure 10. Comparison of experimental Heisenberg spin exchange rate constants using EPR for Cufod in supercritical carbon dioxide to rate calculated by eq 11: (●) $T = 313.1$ K, (○) $T = 308.1$ K, (—) rate constants predicted from eq 11.

can be general, the magnitude of such enhancements can be system-specific. For example, Heitz and Maroncelli[50] found that two out of three solutes investigated followed hydrodynamic theory for rotation in CO_2. However, the two solutes that followed hydrodynamic theory were insoluble below reduced densities of 1.2, well above the low reduced density (0.7) where we see our highest density enhancements.

To examine the possibility that solute−solute local density enhancements could provide an explanation for the slow rotational relaxation of Cufod in near-critical CO_2, we used EPR to measure Heisenberg spin exchange. Heisenberg spin exchange is an unactivated, rapid bimolecular reaction in which two paramagnetic reactants possessing opposite spin-states exchange their spins upon collision.[67] The rate constant, k_e, for spin exchange can be measured by EPR. The rate constant can be predicted from modified Stokes−Einstein theory[67] as

$$k_e = \frac{4kT}{3\eta} f \qquad (11)$$

where f is a steric factor usually assumed to be 1. Figure 10 shows a comparison of the measured rate constant with the one

computed from eq 11. At the lower densities, spin exchange rates are over four times those predicted by Stokes−Einstein theory, and experimental rates do not approach those of theory except at the higher density regions. A likely explanation for the high spin exchange rates is solute−solute local density enhancement. The weak temperature dependence of the observed deviation from theory should also be noted. If solvent critical behavior is responsible for the density enhancement, then a change of 5 K in temperature, especially near to CO_2's critical temperature, would be expected to make a large difference in the observed deviations. The critical temperature of the solute is estimated to be about 1000 K, and five degrees difference in temperature near 300 K should not have a large effect on the results if local density augmentation is dominated by solute−solute interactions. Both our spin exchange data and our lack of temperature dependence indicate that solute−solute interactions should not be neglected in an analysis of rotational correlation times in supercritical fluids.

Conclusions

We report rotational correlation times of Cufod in supercritical carbon dioxide. EPR spectroscopy experiments show that rotational correlation times deviate markedly from those predicted by simple hydrodynamic theory at CO_2 reduced densities of 0.7 to 1.8. When these results are quantified by applying a modified SED equation, it is found that the apparent hydrodynamic radius increases more than 3-fold at lower densities but approaches that found in liquid solvents in the higher, liquidlike density regions. Alternatively, when the model of Anderton and Kauffman[47] is applied to determine local density augmentation, the apparent local densities are more than four times those of the bulk. Although consistent with the results reported by Heitz and Bright,[49] these physically unreasonable values for apparent local densities far surpass those of the liquid solvents. While simulated local densities are monotonic in pressure, experimental values show an unphysical maximum. When local density enhancement is calculated using a Lennard-Jones approach, the local density enhancement is less than that shown experimentally and compares reasonably to liquid densities. A clear maximum for this enhancement is shown for the first time in these types of simulations.

Reaction rate constants for spin exchange from experiments were consistently higher than those predicted by theory, indicating a likely contribution of solute−solute local density enhancements to the observed slowing of molecular rotation in supercritical CO_2. A lack of temperature dependence in our data is also convincing evidence that solute−solute local density enhancements are not a critical phenomenon. These results indicate that solute−solute interactions should not be neglected in models describing rotational correlation times in supercritical fluids.

References and Notes

(1) McHugh, M.; Krukonis, V. *Supercritical Fluid Extraction*; Butterworth: Boston, 1994.

(2) Wu, B. C.; Klein, M. T.; Sandler, S. *Ind. Eng. Chem. Res.* **1991**, *30*, 822.

(3) Brennecke, J. F.; Eckert, C. A. *Proc. Int. Symp. Supercrit. Fluids* **1988**, 263.

(4) Brennecke, J. F.; Eckert, C. A. Fluorescence Spectroscopy Studies of Intermolecular I netractions in Supercritical Fluids. In *Supercritical Fluid Science and Technology*; Johnston, K. P., Penninger, J. M. L., Eds.; American Chemical Society:, Washington, DC, 1989; Vol. 406, pp 14−26.

(5) Coombes, J. R.; Johnston, K. P.; O'Shea, K. E.; Fox, M. A. In *Supercritical Fluid Technology*; Bright, F. V., McNally, M. E. P., Eds., American Chemical Society: Washington, DC, 1992; Vol. 448; p 31.

(6) Betts, T. A.; Zagrobelny, J.; Bright, F. V. In *Supercritical Fluid Technology*; Bright, F. V., McNally, M. E. P., Eds.; 1992; Vol. 448, p 48.

(7) Johnston, K. P.; Kim, S.; Coombes, J. Spectroscopic Determination of Solvent Strenbgth and Structure in Supercritical Fluid Mixtures: A Review. In *Supercritical Fluid Science and Technology*; Johnston, K. P., Penninger, J. M. L., Eds.; American Chemical Society: Washington, DC, 1989; Vol. 406, pp 52−70.

(8) Kajimoto, O.; Futakami, M.; Kobayaski, T.; Yamasaki, K. *J. Phys. Chem.* **1988**, *92*, 1347.

(9) Kim, S.; Johnston, K. P. *Ind. Eng. Chem. Res.* **1987**, *26*, 1206−1213.

(10) Yonker, C. R.; Smith R. D. *J. Phys. Chem.* **1988**, *92*, 235−238.

(11) Carlier, C.; Randolph, T. W. *AIChE J.* **1993**, *39*, 876.

(12) Randolph, T. W.; Carlier, C. *J. Phys. Chem.* **1992**, *96*, 5146−5151.

(13) Brennecke, J. F.; Tomasko, D. L.; Eckert, C. A. *Ind. Eng. Chem. Res.* **1990**, *29*, 1682.

(14) Johnston, K. P.; Haynes, C. *AIChE J.* **1987**, *33*, 2017.

(15) Ganapathy, S.; Randolph, T. W.; Carlier, C.; O'Brien, J. A. *Int. J. Thermophys.* **1996**, *17*, 471−481.

(16) Peck, D. G.; Mehta, A. J.; Johnston, K. P. *J. Phys. Chem.* **1989**, *93*, 4297−4304.

(17) Sun, Y.-P.; Fox, M. A.; Johnston, K. P. *J. Am. Chem. Soc.* **1992**, *114*, 1187−1194.

(18) Nakagawa, K.; Ejiri, A.; Kimura, K.; Nishikawa, M. *Phys. Scripta* **1990**, *41*, 140−142.

(19) Nakagawa, K. *Radiat. Phys. Chem.* **1991**, *5/6*, 643−651.

(20) Cochran, H. D.; Lee, L. L. In *Fluctuation Theory of Mixtures*; Matteoli, E., Mansoori, G. A., Eds.; Taylor and Francis: New York, 1990; p 69.

(21) Cochran, H. D.; Lee, L. L.; Pfund, D. M. *Proc. Int. Symp. Supercrit. Fluids* 1988; Nice, France.

(22) McGuigan, D. B.; Monson, P. A. *Fluid Phase Equilibria* **1990**, *57*, 277.

(23) DeBenedetti, P. G. *Chem. Eng. Sci.* **1987**, *42*, 2203.

(24) Petsche, I. B.; DeBenedetti, P. G. *J. Phys. Chem.* **1991**, *95*, 386−399.

(25) Knutson, B. L.; Tomasko, D. L.; Eckert, C. A.; DeBenedetti, P. G.; Chialvo, A. A. In *Supercritical Fluid Technology*; Bright, F. V., McNally, M. E. P., Eds., American Chemical Society: Washington, DC, 1992; Vol. 448, p 60.

(26) Tucker, S. C.; Maddox, M. W. *J. Phys. Chem.* **1997**, *submitted*.

(27) Randolph, T. W.; Clark, D. S.; W., B. H.; Prausnitz, J. M. *Science* **1988**, *238*, 387−390.

(28) Kazarian, S. G.; Gupta, R. B.; Clarke, M. J.; Johnston, K. P.; Poliakoff, M. *J. Am. Chem. Soc.* **1993**, *115*, 11099.

(29) Gupta, R. B.; Coombes, J. R.; Johnston, K. P. *J. Phys. Chem.* **1993**, *97*, 707.

(30) Debenedetti, P. G.; Chialvo, A. A. *J. Chem. Phys.* **1992**, *97*, 504.

(31) Cochran, H. D.; Lee, L. L. Solvation Structure in Supercritical Fluid Mixtures Based on Molecular Distribution Functions. In *Supercritical Fluid Science and Technology*; Johnston, K. P.; Penninger, J. M. L., Eds.; American Chemical Society: Washington, DC, 1989; Vol. 406, pp 27−38.

(32) Wu, R. S.; Lee, L. L.; Cochran, H. D. *Ind. Eng. Chem. Res.* **1990**, *29*, 977.

(33) Debye, P. *Polar Molecules*; Dover: New York, 1945.

(34) Dote, J. L.; Kivelson, D.; Schwartz, R. N. *J. Phys. Chem.* **1981**, *85*, 2169−2180.

(35) Ahn, M. *Chem. Phys. Lett.* **1977**, *52*, 135.

(36) Basset, A. B. *A Treatise on Hydrodynamics*; Dover: New York, 1961; Vol. 2.

(37) Tanabe, K. *Chem. Phys.* **1978**, *31*, 319.

(38) Perrin, F. *J. Phys. Radium* **1934**, *5*, 497.

(39) Youngren, G. K.; Acrivos, A. *J. Chem. Phys.* **1975**, *63*, 3846.

(40) Gierer, A.; Wirtz, K. *Z. Naturforsch. A* **1953**, *8*, 532.

(41) Evilia, R. F., Robert, J. M.; Whittenburg, S. L. *J. Phys. Chem.* **1989**, *93*, 6550−6552.

(42) Bowman, L. E.; Palmer, B. J.; Garrett, B. C.; Fulton, J. L.; Yonker, C. R.; Pfund, D. M.; Wallen, S. L. *J. Phys. Chem.* **1996**, *100*, 18327−18334.

(43) Howdle, S. M.; Bagratashvili, V. N. *Chem. Phys. Lett.* **1993**, *214*, 215.

(44) Chen, S.; Miranda, D. T.; Evilia, R. F. *J. Supercrit. Fluids* **1995**, *8*, 255−262.

(45) Betts, T. A.; Zagrobelny, J.; Bright, F. V. *J. Am. Chem. Soc.* **1992**, *114*, 8163−8171.

(46) Anderton, R. M.; Kauffman, J. F. *J. Phys. Chem.* **1994**, *98*, 12117−12124.

(47) Anderton, R. M., Kauffman. J. F. *J. Phys. Chem.* **1995**, *99*, 13759−13762.

(48) Reid, R. C.; Prauznitz, J. M.; Poling, B. E. *The Properties of Gases and Liquids*; McGraw-Hill: New York, 1987; pp 424−426.

(49) Heitz, M. P.; Bright, F. V. *J. Phys. Chem.* **1996**, *100*, 6889−6897.

(50) Heitz, M. P.; Maroncelli, M. *J. Phys. Chem. A* **1997**, *101*, 5852−5868.
(51) LaGalante, A. F.; Hansen, B. N.; Bruno, T. J. *Inorg. Chem.* **1995**, *34*, 5781.
(52) Laintz, K. E.; Wai, C. M.; Yonker, C. R.; Smith, R. D. *Anal. Chem.* **1992**, *64*, 2875.
(53) Lemert, R. M.; Fuller, R. A.; Johnston, K. P. *J. Phys. Chem.* **1990**, *94*, 6021−6028.
(54) Lin, Y.; Wai, C. M. *Anal. Chem.* **1994**, *66*, 1971−1975.
(55) Carlier, C., Yale University, 1996.
(56) Schneider, D. J.; Freed, J. H. *Biological Magnetic Resonance*; Plenum Press: New York.
(57) Hathaway, B. J.; Billing, D. E.; Dudley, R. J. *J. Chem. Soc.* **1970**, 1420−1424.
(58) Maki, A. H.; McGarvey, B. R. *J. Chem. Phys.* **1958**, *29*, 31−3233.
(59) Oakes, J. *Nature* **1971**, *231*, 38−39.
(60) O'Brien, J.; Randolph, T. W.; Carlier, C.; Ganapathy, S. *AIChE J.* **1993**, *39*, 1061−1071.
(61) Reid, R. C.; Prauznitz, J. M.; Poling, B. E. *The Properties of Gases and Liquids*, 4th ed.; McGraw-Hill: New York, 1987.
(62) Reid, R. C.; Prausnitz, J. M.; Poling, B. E. *The Properties of Gases and Liquids*; McGraw-Hill: New York, 1987; pp 12−14.
(63) Smit, B., Frenkel, D. *Mol. Phys.* **1989**, *68*, 951−958.
(64) Chi, K. M.; Corbitt, T. S.; Hampden-Smith, M. J.; Kodas, T. T.; Duesler, E. N. *J. Organomet. Chem.* **1993**, *449*, 181.
(65) Ben-Amotz, D.; Scott, T. W. *J. Chem. Phys.* **1987**, *87*, 3739−3748.
(66) Vesovic, V.; Wakeham, W. A.; Olchowy, G. A.; Sengers, J. V.; Watson, J. T. R.; Millat, J. *J. Phys. Chem. Ref. Data* **1990**, *19*, 763−808.
(67) Molin, Y. N.; Salikhov, K. M.; Zamaraev, K. I. *Spin Exchange*; Springer-Verlag: New York, 1980.
(68) Perry, R. H.; Green, D. W. *Perry's Chemical Engineers' Handbook*, 6th ed.; McGraw-Hill: New York, 1984.